

An EmDrive Thruster for Cubesats**Roger Shawyer,***Satellite Propulsion Research Ltd, United Kingdom, sprltd@emdrive.com***Abstract**

Designing an EmDrive thruster for a cubesat presents a number of challenges. Foremost is the need to reduce the size of the microwave cavity, to enable integration into the cubesat structure. This requirement can be addressed by selection of frequency and operating mode.

EmDrive propulsion systems have been designed to operate from 900MHz to around 8 GHz. However, to maintain the low cost cubesat philosophy, a frequency where both components and test equipment are widely available is preferred. The first choice would seem to be the ISM band (2.4GHz to 2.5 GHz). However this leads to cavity sizes which are too big for the largest 12U cubesat structure. The original SPR Flight Thruster was designed around a flight qualified, 3.85 GHz TWTA, and as equipment in the new 5G mobile band (3.4GHz to 3.8GHz) is now readily available, this frequency was also chosen for the cubesat design.

The Flight Thruster had a maximum internal cavity diameter of 200mm, and operated in a TE013 mode. To reduce the maximum diameter to 150mm, the operating mode was changed to TE113. This paper describes the detailed cavity design process, including a description of the design software and the equations used. The resulting cavity dimensions for the cubesat thruster are given, together with E and H field diagrams and plots of wavelength and wave impedance. The placement of input loop, tuner, detector probe and vent are discussed.

The low power available on a typical Cubesat means that the thruster design must utilise the power in the most efficient manner. Essentially this requires that the cavity Q must be maximised. This requirement is addressed in two ways. Firstly the cavity is cooled by using a deployable sunshade, and two deployable cooling panels. Secondly, the end plate alignment, which is critical for high Q and high thrust, is kept within tolerance, by use of the SPR Flight Thruster cavity geometry. A specific thrust of 0.5N/kWm is given for the thruster.

Thrust measurement is described, and the need for a pre-load during thruster start up, using three techniques, are discussed.

The resulting 12U cubesat is described, and tentative missions are proposed, giving a flight time from Low Earth Orbit to a Mars orbit of 8 months, or a time to a Pluto flyby of 4.3 years. Both flight times are within the typical cubesat operational life of 5 years.

Nomenclature K_{nm} Mode constant d_c Cut-off diameter c Speed of light f_0 Resonant frequency λ_{g1} Guide wavelength at large end plate d_1 Diameter of large end plate λ_{g2} Guide wavelength at small end plate d_2 Diameter of small end plate D_f Design factor λ_c Cavity wavelength L_0 Axial length at resonance t Cavity taper λ_{ci} Cavity wavelength increment Z_w Wave impedance E_p E field phase H_p H field phase T Thrust Q_t Theoretical Q value R_s Surface resistance

d_m Mean cavity diameter
 Q_u Unloaded Q value
 Q_i Input circuit Q value
 Q_l Loaded Q value
 D Beam displacement
 W Pre-load weight
 E_s Stored energy
 E_k Kinetic energy

Acronyms/Abbreviations

SSPA Solid state power amplifier
 AU Astronomical unit
 AlMgSi6061 Flight qualified aluminium alloy
 Micron 1Metre x 10^{-6}
 VNA Vector network analyser
 TWTA Travelling wave tube amplifier
 AOCS Attitude and orbit control system
 CW Continuous wave
 LEO Low Earth orbit
 ECU EmDrive control unit
 Delta V Spacecraft velocity change
 LLO Low Lunar orbit
 LMO Low Mars orbit
 SPR Ltd Satellite Propulsion Research Limited

1.Introduction

By describing the design of a cubesat EmDrive thruster, this paper will address four fundamental problems found by numerous research groups attempting to design and manufacture their own EmDrive thrusters. The first problem is simply that EmDrive thrusters will not work successfully unless the microwave cavity is designed correctly. The correct design process requires the solution of the equations for an electromagnetic wave travelling through a waveguide. These equations have been

used by microwave engineers for many decades, to design successful high power radar and other microwave systems. The equations are widely available in standard microwave engineering textbooks, but for a resonant tapered cavity they need to be solved using an incremental method, and then the results are integrated to produce an integer number of half wavelengths. To solve for a fixed mode and operating frequency, the design procedure is inevitably an iterative process. Simply relying on the output of a commercial finite element software package, to give a standing wave solution, can be misleading.

The detailed cavity design process to operate at 3.85GHz in a TE113 mode is given. The design software, based on a widely available spreadsheet package is described, and the equations used are given. The cavity geometry is selected from the three basic circular cavity geometries described in [1]. The critical dimensions resulting from the iterative design process are given. E and H field diagrams and plots of wavelength and wave impedance are presented. The placement of input loop, tuner, detector probe and vent are detailed by reference to the field plots.

Incorrect input tuning and impedance matching is the second common problem found by many research groups. Cavities which simply dissipate all the input power in the input circuit have been found in many cases. To ensure transfer of power to the cavity, the input circuit must be tuned and the impedance matched to the cavity wave impedance, at the resonant frequency, and at the axial position along the cavity. This process requires a two-port method and is why a detector probe is incorporated into the design.

The third problem, is the need to ensure high precision in the critical dimensions which control the path length, and thus phase shift, across the whole area of the wave-front. For a very high Q cavity, and a narrow bandwidth input signal, the machining tolerances need to be measured in microns. The particular geometry selected for the cubesat cavity is the same as that used in the original SPR Flight Thruster [2], and enables the critical dimensions to be mainly determined by flat surfaces, which are easier to machine and measure.

The performance of the thruster, when integrated on a typical 12U cubesat is predicted using the well-established Thrust formula derived in [3]. A 40 Watt solid state amplifier (SSPA) is assumed for powering the thruster. The critical effect of spacecraft thermal design on the thruster performance is discussed, and a

configuration is presented leading to a predicted minimum temperature of -75 degC.

The critical performance parameter of any thruster is of course the thrust which is measured. This leads to the fourth fundamental mistake, made by many research groups, some of whom expect EmDrive to overcome basic physics. EmDrive is an electrical machine, and is therefore subject to the law of the conservation of momentum and the law of the conservation of energy. Conservation of momentum is easily demonstrated by simply placing the thruster on an electronic balance, turning on the thruster, and measuring only noise. This technique has been used for many years to calibrate the noise level in test apparatus, and is described in [2].

Ensuring the test apparatus takes account of conservation of energy is more complex, but means that the dynamic response of the test apparatus must not lead to the rate of increase in kinetic energy of the cavity, being higher than the rate of increase in stored energy, on switch on. This problem, which occurs in extremely sensitive thrust balances, is corrected by providing a pre-load force from the test apparatus. The Thrust/Load theory as described in [1] dictates that a pre-load force must be greater than zero, but less than the predicted thrust, in order to measure thrust successfully. The qualification test programme of any EmDrive flight thruster must demonstrate the capability of overcoming no-load conditions, otherwise the actual mission could be compromised.

The predicted 20mN thrust over a typical 5 year operational life gives enormous scope for planning low cost space tug applications, or science missions throughout the Solar System. However the performance of the solar array means that most of the acceleration must take place within the normal 1AU operating range for cubesats.

2.Cavity Electrical Design

The initial input data for calculating the electrical design of the cavity are:

Mode

Resonant Frequency

Small endplate diameter

Large end plate diameter

Table 1 gives the values of K_{nm} for lower order TE modes in a circular waveguide. The derivation of K_{nm} is given in [4].

n	1	2
0	0.82	0.448
1	1.706	0.589
2	1.029	0.468

Table 1.

Thus TE11 is seen to have the highest value of K_{nm} and therefore this mode will yield the smallest cut off diameter d_c as given by:

$$d_c = \frac{\lambda_0}{K_{nm}} \quad (1)$$

Where λ_0 is the free space wavelength

The free space wavelength λ_0 is given by:

$$\lambda_0 = \frac{c}{f_0} \quad (2)$$

Where c = speed of light, taken as 2.99705543×10^8 m/s, and f_0 = resonant frequency in Hz.

Clearly the small end plate diameter must be above the cut off diameter, with a small margin for machining tolerance and operating temperature range.

The guide wavelengths at the large and small end plates are given by:

$$\lambda_{g1} = \frac{\lambda_0}{\sqrt{1 - \left(\frac{\lambda_0}{K_{nm}d_1}\right)^2}} \quad (3)$$

where d_1 = diameter of large end plate

$$\lambda_{g2} = \frac{\lambda_0}{\sqrt{1 - \left(\frac{\lambda_0}{K_{nm}d_2}\right)^2}} \quad (4)$$

where d_2 = diameter of small end plate

The diameter of the large end plate should be as large as practical, as this maximises the design factor D_f , where:

$$D_f = \frac{\frac{\lambda_0}{\lambda_{g1}} \frac{\lambda_0}{\lambda_{g2}}}{1 - \left(\frac{\lambda_0^2}{\lambda_{g1}\lambda_{g2}}\right)} \quad (5)$$

The derivation of D_f is given in [5].

To calculate the axial length of the cavity, the number of half wavelengths must be chosen. This number should be minimised, but consistent with ensuring minimum distortion of the field structure due to the

input element. For a sidewall loop input, 3 half wavelengths have been found to be optimum.

Thus the cavity wavelength $\lambda_c = 1.5$

The axial length of the cavity is found by numerical integration of the increasing incremental guide wavelength, from the large end plate, until an overall value of 1.5 is achieved for the cavity wavelength. This is carried out using spreadsheet software where the columns are defined in Table 2.

Column	Equation	Description
A	$L = An + 0.1$	Increments axial length L by 0.1mm
B	$d = d_n - \frac{t}{10}$	Increments diameter according to taper t
C	$\lambda_g = \frac{\lambda_0}{\sqrt{1 - \left(\frac{\lambda_0}{K_{nm}d}\right)^2}}$	Calculates guide wavelength at diameter d
D	$\lambda_{ci} = \frac{0.1}{\lambda_g}$	Calculates cavity wavelength increment
E	$\lambda_c = \lambda_{ci} + \lambda_{c(n-1)}$	Cavity wavelength integrated over axial length 0 to L
F	$Z_w = 376.7 \sqrt{1 - \left(\frac{\lambda_0}{K_{nm}d}\right)^2}$	Calculates wave impedance at diameter d
G	$E_p = \frac{d}{2} \sin(2\pi \lambda_c)$	Plots E field phase
H	$H_p = \frac{d}{2} \cos(2\pi \lambda_c)$	Plots H field phase

Table 2

Each line of the spreadsheet is a 0.1mm increment in axial length.

The design process is iterative with an initial axial length selected to determine the taper t where:

$$t = \frac{d_1 - d_2}{L_0} \quad (6)$$

where L_0 = axial length at resonance

The axial length is successively changed until the cavity wavelength closely approaches 1.5. Final iteration can be carried out by small changes to the resonant frequency.

3. Electrical Design Results

Using the equations and the design process described in section 2, the cavity electrical design results for the cubesat thruster are:

Large end plate internal diameter = 150mm

Small end plate internal diameter = 48mm

Axial length at resonance = 140mm

Resonant frequency = 3858.3 MHz

Cut off diameter = 45.53mm

Design factor = 0.911

A plot of guide wavelength against axial length is given in Fig.1 and a plot of cavity wavelength in Fig.2

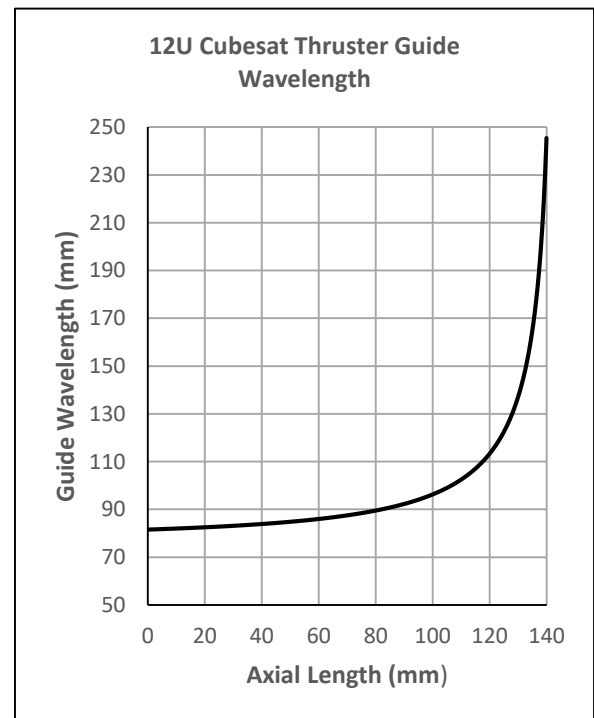


Fig.1

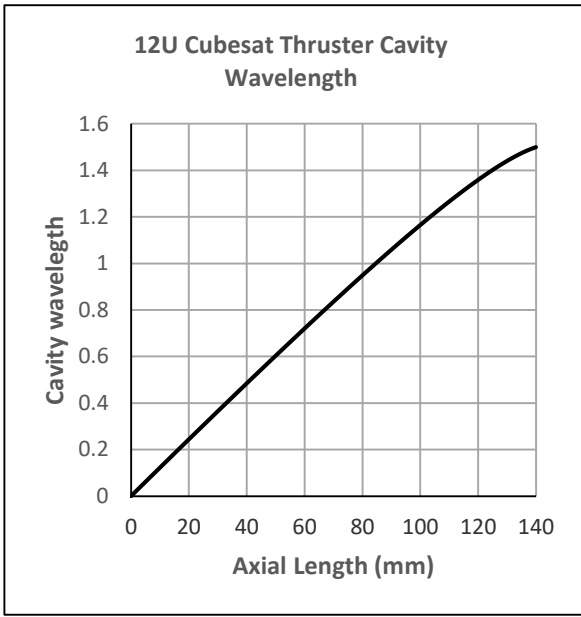


Fig.2

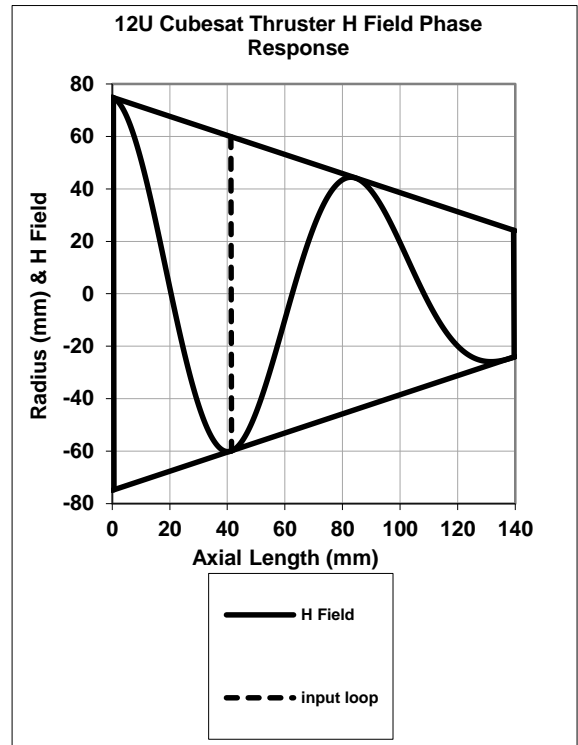


Fig.4

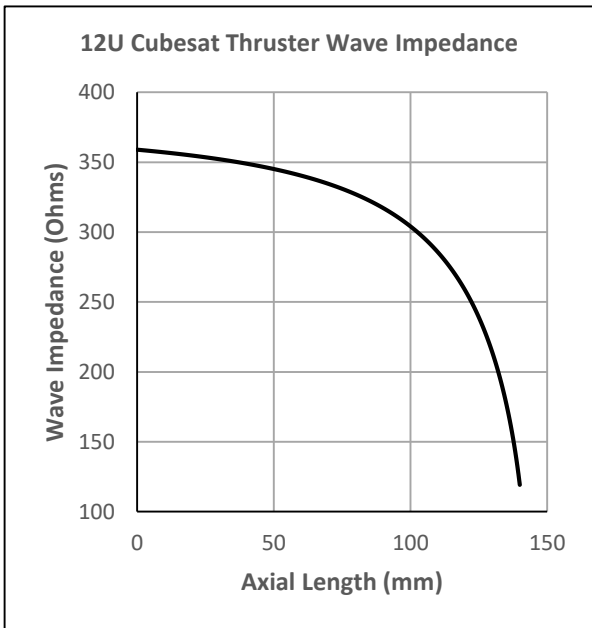


Fig.3

A plot of wave impedance against axial length is given in Fig.3

To help to visualise the H and E fields, their phase response is plotted within the cavity outline as shown in Figs. 4 and 5. The positions of the input loop at an H field maximum, the detector probe at an E field maximum and the vent-hole, at an E field minimum, are also shown.

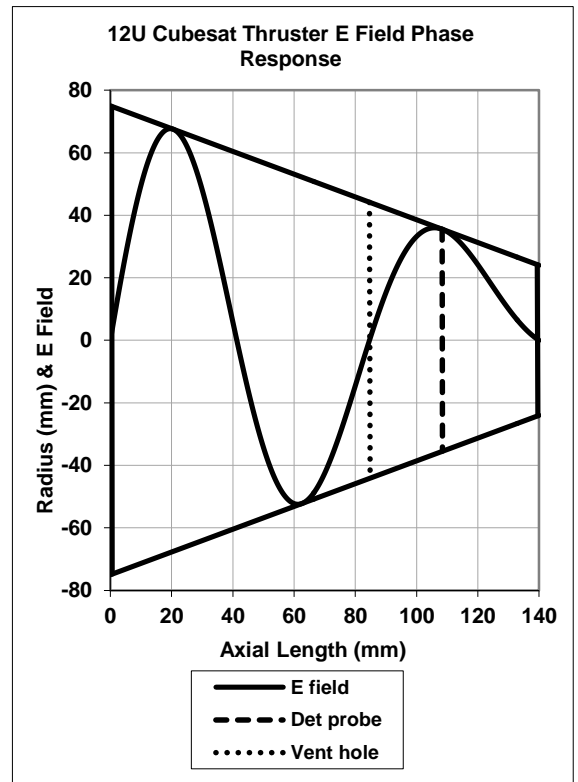


Fig.5

The axial lengths at which the input loop, detector probe and vent-hole are positioned, are given in Table 3.

Wave impedances, to allow matching for the input loop and detector probe, are also given. The input loop, input tuner and detector probe are similar to those described in [2] for the Flight Thruster, but modified for the cubesat cavity impedances.

Component	Axial Length (mm)	Cavity Wavelength	Wave Impedance (Ohms)
Input Loop	41.3	0.5	348.5
Vent-hole	84.7	1.0	322.7
Detector Probe	108.4	1.25	289.1

Table 3

It is critical that the input circuit is not just tuned to match the power source, which in this case is the 50 Ohm output of an SSPA but that it also matches the wave impedance of the cavity. The wave impedance varies with position along the axial length of the cavity as shown in Fig.3.

4. Cavity Geometry

The design software assumes both end plates are flat. In practice this geometry would result in a low Q value as the actual path length will increase as the path approaches the side wall from the central axis, due to the taper. A number of geometries can be used to overcome this problem, and three are described in [1]. To retain simplicity for the cubesat application, the same geometry as that used for the original Flight Thruster is retained.

Other geometries using spherical or complex curves require active alignment systems to obtain maximum Q values, and it is considered that the use of piezo-electric elements and a digital control system is not necessary for the geometry described, and the cost and complexity not warranted for a cubesat application.

The cubesat geometry is shown in Fig.6, and comprises a flat small end plate, with the large end plate having a central flat face, and an annular section, with a radius equal to the central axial length. This allows the alignment of the two end plates to be

mainly controlled by the surface flatness of the small end plate, the central section of the large end plate and the flange surfaces of the plates and body section. Surface flatness can generally be held to higher tolerances than those specified for curved surfaces.

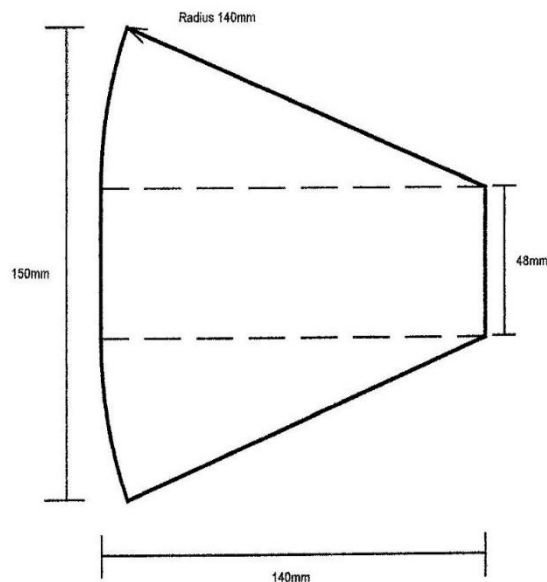


Fig.6

End plate misalignment results in low Q values, and disproportionately low thrust performance [1]. The alignment process, either grinding of the flange or flat end plate surfaces, or by use of shims between the flange faces, can be assisted by the monitoring of the Q values of the multiple fixed cavity resonance peaks, that result from misalignment.

As for the Flight Thruster, the cavity is machined from AlMgSi 6061 alloy, with inner surfaces silver plated to flight specification.

5. Thruster Performance

The thrust of an EmDrive thruster is given in [5] by:

$$T = \frac{2PQ_u S_0}{c} \left[\frac{\lambda_0}{\lambda_{g1}} - \frac{\lambda_0}{\lambda_{g2}} \right] \quad (7)$$

$$\text{Where } S_0 = \left[1 - \frac{\lambda_0^2}{\lambda_{g1}\lambda_{g2}} \right]^{-1} \quad (8)$$

The theoretical Q of a circular cavity in TE mode is given in [4] by:

$$Q_t = \frac{\left(\frac{377}{2R_s}\right) \left[14.684 + \left(\frac{1.571p d_m}{L_0}\right)^2\right]^{1.5}}{14.684 + \left[\frac{d_m \left(\frac{1.571p d_m}{L_0}\right)^2}{L_0}\right]} \quad (9)$$

Where R_s is the surface resistance of silver at f_0

And d_m is the mean diameter of the cavity.

The theoretical Q_t for the cubesat cavity is calculated to be 87,958

However the actual Q_u will be reduced by the alignment error.

Assuming a 20 micron overall alignment error, then from Flight Thruster data [2], the predicted Q_u for the cubesat cavity will be 84,064.

To ensure maximum transfer of input power into the cavity, the input circuit must be impedance matched to the cavity impedance, at the axial length of the input, and at the correct resonant frequency for the operating temperature of the cavity.

Also the Q of the tuned input circuit Q_i must equal the unloaded Q of the cavity Q_u to satisfy the equation:

$$\frac{1}{Q_l} = \frac{1}{Q_i} + \frac{1}{Q_u} \quad (10)$$

Where Q_l is the loaded Q of the cavity.

Thus for correct input circuit matching, the measured Q_l will be half the unloaded Q_u .

To obtain the correct match in each direction, (i.e. source and cavity), a two port measurement is required, using the detector probe output and a measurement of either input power or reflected power. During the tuning process it is possible to display the two resonant peaks of the cavity (detector power) and the input circuit, (input power), by use of a dual channel Vector Network Analyser, (VNA). With suitable scaling, the input circuit peak can then be moved to coincide with the fixed cavity peak, by use of the tuning element. Optimum tuning is achieved when both peaks exactly coincide, with the same Q values.

Care must be taken not to confuse the input circuit peak, with other fixed cavity peaks which can occur due to cavity end plate misalignment, (see section 4).

Then for 40W power inside cavity, the calculated Thrust $T=20.44\text{mN}$.

6. Thrust Measurement

To measure EmDrive thrust, the apparatus used must take account of the conservation of momentum and the conservation of energy. EmDrive is not a conventional rocket engine and therefore, although thrust can be measured on a variety of conventional balances, beam, pendulum or torsional, the measurement technique must include application of a pre-load. It is also considered important to prepare a numerical model of the dynamic response of the balance, in order to fully understand the results of the thrust measurement.

To illustrate this, consider an ideal beam balance as shown in Fig.7.

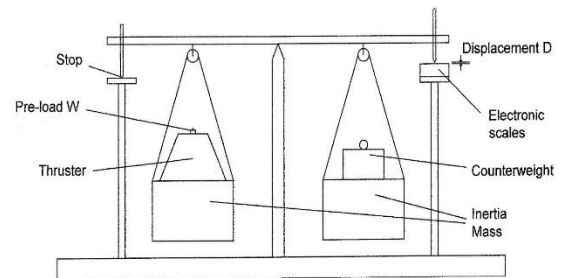


Fig.7 Ideal Beam Balance

Assume the weight of the thruster is exactly balanced by counterweights, and the beam is held against a stop by a pre-load weight, designated W. Assume there is no friction at the pivot point and the total mass of the beam, thruster and counterweights presents an inertial load along the thrust axis equal to the spacecraft mass of 20kg. An electronic balance is positioned below the counterweight side of the beam, with a clearance set to be greater than expected maximum beam displacement D.

Note that whichever type of balance is chosen, the need to transfer power, either DC or microwave, from the fixed to the moving parts of the balance, without causing spurious forces is critical. The beam balance used for testing the Flight Thruster incorporated a free waveguide coupling described in [2], which allowed up to 500W of microwave power to be transferred from a TWTA to the thruster, with low spurious force levels.

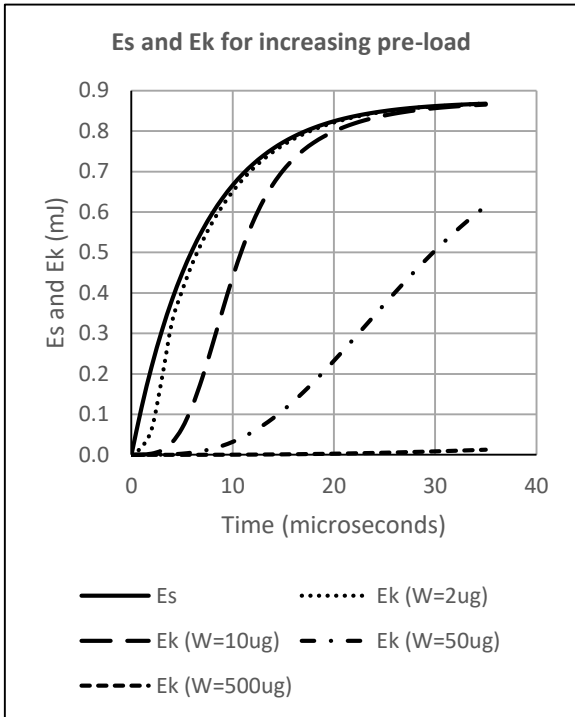


Fig.8

This ideal balance has been modelled for the predicted Q_u and thrust of the cubesat thruster, and the stored energy and kinetic energy are shown in Fig. 8, for the first 35 microseconds after switch on. This period represents five times the time constant of the cavity, during which the stored energy E_s rises exponentially to a maximum value.

The kinetic energy of the total inertial load is shown in Fig.8, for increasing pre-loads, designated W , from 2 micrograms to 500 micrograms. Clearly at a pre-load of 2 micrograms, the increase in kinetic energy is close to the increase in stored energy once the initial square law rise is modified by the inertial load.

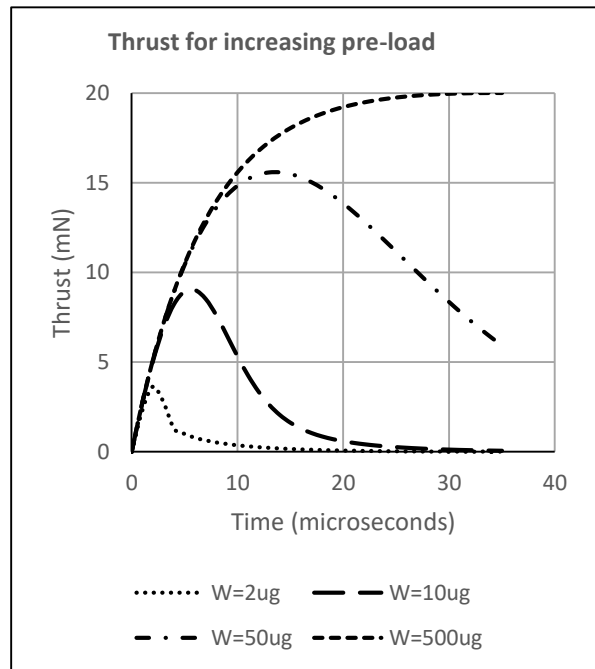


Fig.9

The corresponding thrust response, for a pre-load of 2ug, shown in Fig.9, gives a small peak during the initial 5 microseconds when stored energy is slightly above kinetic energy. Thrust then drops to zero, as kinetic energy closely follows the rise in stored energy, thus leaving the net energy, available for generating thrust, approaching zero. No constant measurement of thrust will be possible at these low pre-load values, although the pre-loads may be higher than the resolution possible in very sensitive thrust balances.

As the pre-load is increased, the initial acceleration of the beam drops, the rise in kinetic energy is reduced, and more net energy is available to produce thrust. At a pre-load above 500 micrograms, i.e. a force of 5 micro-Newtons, constant thrust will be measured, once the beam displacement is sufficient to reduce the electronic balance clearance to zero.

The predicted beam displacement during the first 35 microseconds is given in Fig.10.

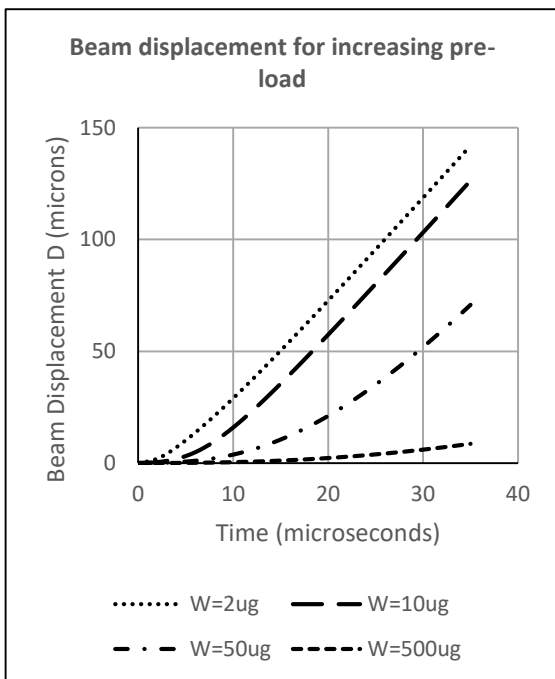


Fig.10

7. Integration of thruster on a cubesat

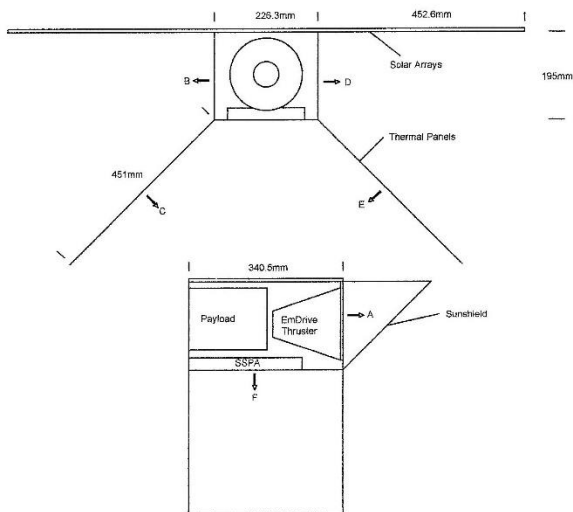


Fig. 11 Cubesat Outline

The positioning of the thruster within the cubesat structure must take account of both mechanical and thermal considerations. Clearly for primary propulsion, the thrust axis, which is the central axis of the thruster, should be closely aligned with the

centre of mass and the Z axis of the satellite. The overriding thermal requirement is to reduce the operating temperature of the thruster, to minimise resistance of the silver inner surface of the cavity, and thus maximise the Q value. An outline diagram of the thruster together with a 40W SSPA integrated on a typical 12U cubesat is given in Fig.11.

Note that the SSPA could be incorporated into the telemetry transmission system. This would give a very high power signal, with consequent high data rates, or very long range, for deep space science missions.

The satellite carries thermal radiating panels, A, B, C, D and E, to reduce the operating temperature of the thruster, which will dissipate a maximum of 40Watts. The A panel is shaded using a lightweight deployable sunshield, whilst the other panels are shaded by the solar arrays. Panels C and E are deployable. Under full shade, the temperature of the thruster would reduce to -75 deg C. The SSPA is thermally isolated from the thruster and is cooled by panel F to a maximum operating temperature of 61 deg C, whilst dissipating 52W. Panel F is shaded by the main body of the satellite.

A preliminary mass budget for the cubesat is given in table 4, where a margin of 10% is added, as most of the equipment is already flight qualified. To keep below a launch mass of 20kg, a payload mass of 6 kg is allocated.

Item	Mass (kg)
Cubesat structure	1.386
Solar panel	0.932
Array structure	2.311
Power conditioner	0.148
Battery	0.67
Frequency generator	0.019
SSPA	0.856
Attitude control	1.135
Telemetry & command	0.1
EmDrive cavity	2.4
EmDrive control unit	0.3
Cabling	0.2
Thermal structure	2.233
10% contingency	1.269
Payload	6
Total	19.959

Table 4. Mass budget

8. Flight Operations

Clearly there are some operational situations where the thruster may have to start up with no pre-load. A cubesat with only one thruster and a simple Attitude and Orbit Control System (AOCS) will need to adopt additional techniques to provide the necessary initial pre-load. Pulsed input power, as described in [1], will reduce the problem.

However, to optimise power system and SSPA mass, the SSPA and thruster should be run in CW mode, and so the preload would be applied as a mechanical pulse. A momentum wheel can be used to induce a pitch or yaw movement, which will produce a centrifugal force on the cavity. For this to be effective, the thruster must be positioned along the Z axis, with sufficient separation from the spacecraft centre of mass. An initial mass properties analysis gives this radius as 146mm, which means the required pre-load of 5uN can be obtained with a slew rate of .07degs/s. This is well within the typical maximum slew rate for cubesats.

Use of gravity loading whilst in LEO, can also be applied, as in the Lunar mission described in [1]. In this case the cubesat would be oriented with the z axis aligned to the Earth's gravity vector, with the cavity mass below the centre of mass of the cubesat. The pre-load force obtained from the gravity gradient within the cubesat is shown in Fig. 12. Up to an orbital altitude of 1,800km, the gravity gradient will produce a continuous pre-load force above 5 uN.

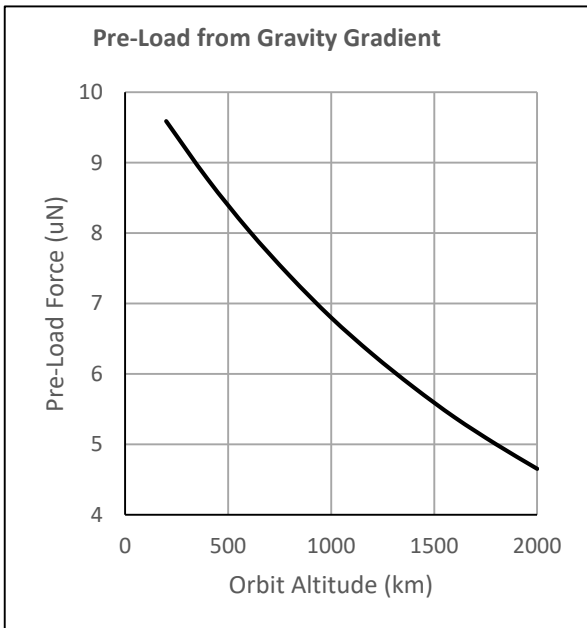


Fig.12

Alternatively, to avoid use of the AOCS system, a small solenoid, with the body fixed to the spacecraft structure and the armature free to move, can be used. The solenoid stroke is aligned along the thrust axis. The solenoid is pulsed as the thruster is switched on, and the armature momentum is mechanically transferred to the thruster through the spacecraft structure. This mechanical impulse provides a pre-load force pulse, whilst the armature is moving, and the Qu and thrust will continue to build up in this period. Once this start-up impulse is complete, the momentum is reversed, but the inertial load of the accelerating spacecraft ensures thrust is maintained. The solenoid can then be switched off, returning the armature to its original position. A typical solenoid can transfer an average pre-load force of 5 uN to the spacecraft, over a period of 10 msecs, for an input power of 2W. A solenoid pre-load force profile is shown in Fig.13.

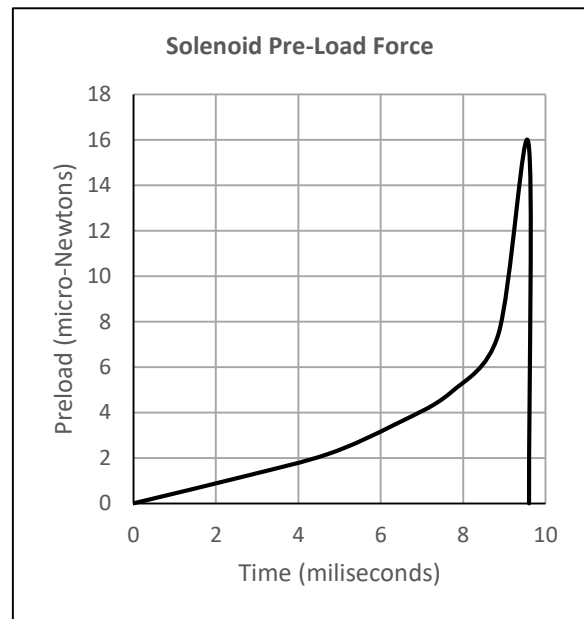


Fig.13

The solenoid is incorporated in the EmDrive Control Unit (ECU), which also includes a frequency generator circuit and a processor to control the thruster input frequency, from the feedback of power and temperature monitoring circuits. Start-up frequency sequencing, to optimise frequency for the differing temperature profiles of the cavity and input circuit is essential, and is controlled by the processor. A sweep function is also included to enable Q measurements to be made as part of routine

performance monitoring. Thruster telemetry and command functions are routed through the ECU.

9. Potential Missions

The design presented above results in a 20kg spacecraft propelled by a thruster which provides 20mN of continuous thrust. Assuming constant illumination of the solar arrays, this level of thrust can be maintained over a typical cubesat specified operating lifetime of 5 years. A maximum terminal velocity of 160km/s is therefore possible.

The first mission application to be considered is the use of the cubesat as a space tug for small satellites. If the payload is a 50kg satellite, a total delta V of 46 km/s can be achieved. This can be compared to a delta V of only 1 km/s for the same payload, which is the limit of the existing best small electric space tug performance, using microwave power and water propellant. Clearly with this huge improvement in performance, with a suitable docking mechanism, the EmDrive propelled cubesat could carry out multiple space tug missions in Earth orbit, or in lunar transfer missions.

For transfer from LEO to Low Lunar Orbit (LLO) of a 100kg satellite, an outward flight time of 18 months is required. With a return flight time of 3 months, three transfer missions are possible within the 5 year operational life, assuming the 20kg cubesat is left in LLO on the third mission. This can again be compared with a microwave and water propelled spacecraft, which would weigh 450kg, and would only manage a single transfer, taking 10 months.

Two deep space missions illustrate the flight times possible for an EmDrive propelled cubesat. The first is a flight from LEO to a low Mars orbit (LMO). The flight starts with a spiral out of LEO to a Mars transfer orbit, taking 64 days. A direct transit is followed with acceleration to mid-point and then deceleration to Mars capture. This takes 152 days, during which the spacecraft reaches a maximum velocity of 11km/s. Mars capture takes a further 10 days and is followed by a spiral down to LMO of 21 days. The estimated total mission time is based on a total delta V requirement of 6.6km/s, and mean eclipse periods of 0.32%, and results in a flight time of 8.1 months.

However the true potential of EmDrive for deep space missions, is illustrated by the possibility of a Pluto flyby mission within a 5 year total flight time. Such deep space missions need to maintain acceleration periods within 1AU distance from the

Sun to provide nominal solar array performance. The mission profile thus becomes a slow spiral out of LEO, an acceleration period in multiple Sun orbits, plus a cruise period at a constant terminal velocity. Fig. 14 gives the result of a simple mission optimisation, to give a minimum total mission time of 4.3 years, for an acceleration period of 2 years and a terminal velocity of 63km/s.

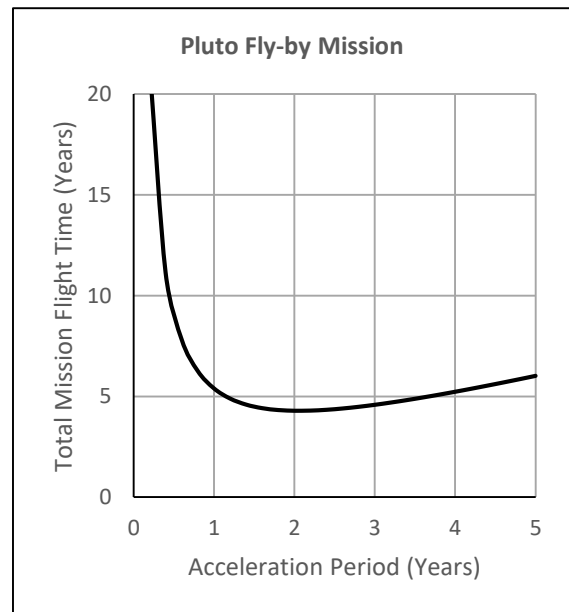


Fig.14

10. Conclusions

This paper has given the first detailed description of the design process used for the successful design of an EmDrive thruster. The description includes all the design equations, and details of the spreadsheet design tool developed by SPR Ltd, and used for many successful thruster designs.

The paper includes discussion of other basic knowledge that is essential to produce a working thruster. This includes the impedance matching, tuning and alignment. Also reference is made to the fact that EmDrive is an electrical machine, and test apparatus must take account of EmDrive complying with the principles of the conservation of momentum, and the conservation of energy.

The design example chosen is a thruster which can be integrated into a 12U cubesat.

The result is a low cost, 20kg spacecraft, with a continuous thrust of 20mN.

Three mission examples are given, a space tug for Earth orbit or lunar transfer, a transfer to Mars orbit and a fly-by of Pluto.

The use of EmDrive propulsion therefore opens up the possibility of low cost, cubesat missions, throughout the whole Solar System.

References

- [1] R.J.Shawyer, EmDrive Thrust/Load Characteristics. Theory, Experimental Results and a Moon Mission, IAC-19-C4.10.14, 70th International Astronautical Congress, Washington DC, 21-25 October 2019.

- [2] Report on the Design Development and Test of a C-Band Flight Thruster, September 2010. Issue 2, December 2017. SPR Ltd Available on www.emdrive.com

- [3] R.J.Shawyer, Microwave Propulsion – Progress in The EmDrive Programme. IAC-08-C4.4.7. 59th International Astronautical Congress, Glasgow UK, 29th September-3rd October 2008.

- [4] P.A.Rizzi, Microwave Engineering Passive Circuits, Prentice-Hall, New Jersey 1988.

- [5] R.J.Shawyer, A Theory of Microwave Propulsion for Spacecraft V9.4, SPR Ltd, 2006. Available on www.emdrive.com